Analysis of Femto Base Station Network Deployment

YungLan Tseng and ChingYao Huang, *Member, IEEE*

***Abstract*—In this paper, assurance of proper downlink outage probability, which is a design criterion based on feasible femto base station (BS) density, is analyzed. Considering femto BS deployment, a 3-D Poisson model of random spatial distribution and stochastic geometry are used. From the study, a closed form of feasible femto BS density will be identified. The analysis results not only can be used to predict the performance of various femto BS deployment scenarios but also can be used as a design criterion for resource control mechanism designs.**

***Index Terms*—Femto base station (BS), stochastic geometry, wireless networks.**

I. Introduction

FEMTO base stations (BSs) have been proposed in both WiMAX [1] and long-term evolution systems [2] to improve indoor data rates and extend cell coverage [3], [4]. However, the benefit of deploying femto BSs will be affected by access modes and deployment scenarios.

According to [2], a femto BS has three different access modes: 1) closed subscriber group (CSG); 2) open access [which is known as an open subscriber group (OSG)]; and 3) hybrid access. A CSG consists of a set of subscribers authorized by the femto BS owner or service provider. The CSG femto BS supports only its CSG users. On the contrary, the open access femto BS supports all users within its coverage. A hybrid femto BS supports both CSG and non-CSG users, although the non-CSG users have only limited access. Apparently, femto BSs will have different interference impacts on surrounding environments if the associated access modes are different.

In addition to access modes, femto BSs, which are randomly deployed by users, will potentially generate undesired interference that could degrade the overall performance of the femto BS network [4]. Furthermore, femto BSs would also interfere with macro BS users when both are colocated and share the same spectrum [4]. To reduce these interference problems, there are extensive studies that try to eliminate interference through power control [5]–[7], spectrum allocation [8], [9], and scheduling [1], [10]. However, these studies did not consider the influence of random deployment. To account for this influence, stochastic geometry [11]–[14] has been applied to femto BS or *ad hoc* networks for BS/node distribution. In [15], Poisson shot noise was applied to resource allocation between macro BS and femto BS networks. In [16], Weber and Andrews calculated the upper and lower bounds of the outage probability in an ad hoc network by assuming that all interfering nodes follow a homogeneous Poisson point process (HPPP). From [16], it observes that a major interference node will dominate the lower bound of the outage probability. Furthermore, Mordachev and Loyka [17] also found that the outage probability is largely determined by the dominant interference node when the network is operated at low outage probability and the locations of interfering nodes obey an HPPP.

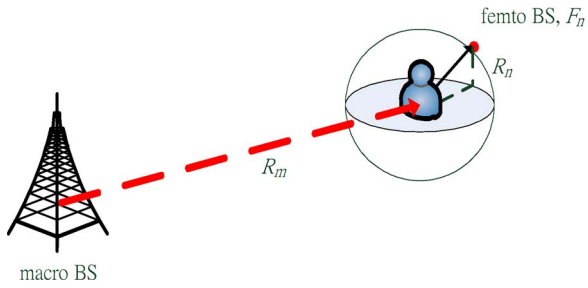

Fig. 1. Femto BS network analysis model. R_m is the distance between the user and the macro BS. R_n is the distance between the user and its nth nearest femto BS F_n.

In this paper, we will investigate the influence of active femto BSs in the downlink direction and estimate the feasible femto BS density for a target threshold of outage probability. In our study, the femto BS density is infeasible when the associated outage probability is higher than the target threshold decided by a prior decision. The analysis model will be based on the following assumptions: 1) a 3-D analysis model to reflect the condition that interference comes from all directions [18]; 2) stochastic geometry to analyze the influence of random deployment; and 3) a dominant interference node to be used to approximate the overall outage probability [17].

The rest of this paper is arranged as follows: In Section II, we construct an analysis model to analyze the user's signal-to-interference ratio (SIR). In Section III, feasible solutions and theorems of the femto BS deployment density based on the analysis model are proposed. In Section IV, simulations are constructed to verify the proposed theorems. In Section V, we will discuss how to implement our observations in the femto BS deployments and control mechanisms. Finally, in Section VI, we summarize the observations and contributions of this study.

II. Analysis Model

Our analysis model is constructed in 3-D space, as plotted in Fig. 1, in which, aside from having a conventional macro BS

Manuscript received December 12, 2010; revised May 11, 2011 and September 15, 2011; accepted October 16, 2011. Date of publication November 16, 2011; date of current version February 21, 2012. The review of this paper was coordinated by Prof. H. Liu.

The authors are with the Department of Electronics Engineering and Institute of Electronics, National Chiao Tung University, HsinChu 300, Taiwan (e-mail: bravery8126.ee96g@g2.nctu.edu.tw; cyhuang@mail.nctu.edu.tw).

Color versions of one or more of the figures in this paper are available online at http://ieeexplore.ieee.org.

Digital Object Identifier 10.1109/TVT.2011.2176355

TABLE I
CLOSED FORMS UTILIZED IN THE INTEGRAL TERMS OF $E[\ln(R_n)]$

n	$\int \ln(x)x^{3n-1}\exp(-cx^3)dx$
1	$(9c)^{-1}(\mathrm{Ei}(-cx^3)-3\exp(-cx^3)\ln(x))$
2	$(9c^2)^{-1}\exp(-cx^3)(\exp(cx^3)\mathrm{Ei}(-cx^3)-3(cx^3+1)\ln(x)-1)$
3	$(9c^3)^{-1}\exp(-cx^3)(2\exp(cx^3)\mathrm{Ei}(-cx^3)-3(c^2x^6+2cx^3+2)\ln(x)-cx^3-3)$
4	$(9c^4)^{-1}\exp(-cx^3)(6\exp(cx^3)\mathrm{Ei}(-cx^3)-3(c^3x^9+3c^2x^6+6cx^3+6)\ln(x)-c^2x^6-5cx^3-11)$
5	$(9c^5)^{-1}\exp(-cx^3)(24\exp(cx^3)\mathrm{Ei}(-cx^3)-3(c^4x^{12}+4c^3x^9+12c^2x^6+24cx^3+24)\ln(x)-c^3x^9-7c^2x^6-26cx^3-50)$
6	$(9c^6)^{-1}\exp(-cx^3)(120\exp(cx^3)\mathrm{Ei}(-cx^3)-3(c^5x^{15}+5c^4x^{12}+20c^3x^9+60c^2x^6+120cx^3+120)\ln(x)-c^4x^{12}-9c^3x^9-47c^2x^6-154cx^3-274)$
7	$(9c^7)^{-1}\exp(-cx^3)\begin{pmatrix}720\exp(cx^3)\mathrm{Ei}(-cx^3)-3(c^6x^{18}+6c^5x^{15}+30c^4x^{12}+120c^3x^9+360c^2x^6+720cx^3+720)\ln(x)-c^5x^{15}-11c^4x^{12}-74c^3x^9\\-342c^2x^6-1044cx^3-1764\end{pmatrix}$

and a user, with the density of λ, femto BSs are assumed to be uniformly distributed around the user. By considering a user located at the center of a sphere space, the surrounding number of femto BSs will follow HPPP [11]–[13]. Furthermore, its probability density function (pdf) can be represented by

$$\Pr_X(x,\lambda,\upsilon)=(\lambda\upsilon)^x\exp(-\lambda\upsilon)/x!,\qquad \upsilon=4\pi r^3/3. \quad (1)$$

Here, x is the number of femto BSs in the sphere, and r and υ are the radius and volume of the sphere, respectively. The pdf of R_n, $\Pr_{R_n}(r)$, can be calculated from $\Pr_X(x,\lambda,\upsilon)$, as shown in

$$\begin{aligned}\Pr_{R_n}(r)&=\partial\left(1-\Pr(R_n\geq r)\right)/\partial r, \Pr(R_n\geq r)\\&=\sum_{x=0}^{n-1}\Pr_X(x,\lambda,\upsilon)\\&=\sum_{x=0}^{n-1}(4\pi\lambda r^3/3)^x\exp(-4\pi\lambda r^3/3)/x!. \quad (2)\end{aligned}$$

Therefore, $\Pr_{R_n}(r)$ obeys the generalized Gamma distribution [19].

$$\Pr_{R_n}(r)=\frac{3(4\pi\lambda r^3/3)^n}{r\Gamma(n)}\exp(-4\pi\lambda r^3/3). \quad (3)$$

Here, $\Gamma(n)$ is the Gamma function. By considering the transmitted power and path-loss impacts, the received signal strength U_n can be calculated by [20]

$$U_n=P_{fn}-\delta_{fn}-10\eta_f\log_{10}(R_n)\ (\mathrm{dB}),\qquad R_n\geq\varepsilon \quad (4)$$

where P_{fn} is the transmission power of femto BS, F_n, and δ_{fn} is the path-loss constant between user and F_n. η_f is the path-loss exponent of femto BS networks, and ε is assumed to be small and can be ignored.

For calculating U_n, we need to obtain the pdf of $\ln(R_n)$. Here, we define $Z_n\equiv\ln(R_n)$, and the pdf of Z_n can be calculated from $\Pr_{R_n}(r)$, i.e.,

$$\begin{aligned}&\Pr_{Z_n}(z_n)\equiv\Pr_{R_n}(\exp(z_n))\,|\partial R_n/\partial z_n|, \ln(\varepsilon)\leq z_n\leq\infty\\&\Rightarrow\Pr_{Z_n}(z_n)=\frac{3(4\pi\lambda\exp(3z_n)/3)^n}{\Gamma(n)}\\&\qquad\times\exp\left(-4\pi\lambda\exp(3z_n)/3\right). \quad (5)\end{aligned}$$

Note that $\Pr_{Z_n}(z_n)$ is an approximation because we assume $R_n\geq\varepsilon$. However, this would not detract from the conclusion of this paper because $\Pr(R_n<\varepsilon)$ is very small.

From (4), it is clear that, to calculate the expected value of the received signal strength from F_n, i.e., $E[U_n]$, $E[\log_{10}(R_n)]$ needs to be calculated first. We will calculate $E[\log_{10}(R_1)]$ first and then extend to $E[\log_{10}(R_n)]$, i.e.,

$$\begin{aligned}&E\left[\log_{10}(R_1)\right]\\&\quad=E\left[\ln(R_1)\right]/\ln(10)\\&\quad=(4\pi\lambda/\ln(10))\cdot\int_{\varepsilon}^{\infty}\ln(r)r^2\exp(-4\pi\lambda r^3/3)dr. \quad (6)\end{aligned}$$

From Table I [21], the integral term can be transformed as

$$\begin{aligned}&\int_{\varepsilon}^{\infty}\ln(r)r^2\exp(-4\pi\lambda r^3/3)dr\\&\quad=\left.\frac{\mathrm{Ei}(-cr^3)-3\exp(-cr^3)\ln(r)}{9c}\right|_{\varepsilon}^{\infty}\\&\quad=\frac{\mathrm{Ex}(c\varepsilon^3)+3\exp(-c\varepsilon^3)\ln(\varepsilon)}{9c}\\&\quad\approx\frac{\mathrm{Ex}(c\varepsilon^3)+3\ln(\varepsilon)}{9c},\qquad c=\frac{4\pi\lambda}{3}. \quad (7)\end{aligned}$$

Here, $\mathrm{Ei}(z)$ and $\mathrm{Ex}(z)$ are exponential integrals, i.e.,

$$\mathrm{Ei}(z)\equiv\int_{-\infty}^{z}\exp(t)/t\,dt\quad\mathrm{Ex}(z)\equiv\int_{z}^{\infty}\exp(-t)/tdt$$

$$\mathrm{Ei}(-z)=-\mathrm{Ex}(z). \quad (8)$$

TABLE II
CLOSED FORMS OF $E[\ln(R_n)]$

R_n	PDF of R_n	E[ln(R_n)]
R_1	$4\pi\lambda r_1^2 \exp(-4\pi\lambda r_1^3/3)$	$(-\gamma-\ln(4\lambda\pi/3))/3$
R_2	$(16/3)\pi^2\lambda^2 r_2^5 \exp(-4\pi\lambda r_2^3/3)$	$(-\gamma-\ln(4\lambda\pi/3))/3+(1/3)=\mathrm{E}[\ln(R_1)]+(1/3)$
R_3	$(32/9)\pi^3\lambda^3 r_3^8 \exp(-4\pi\lambda r_3^3/3)$	$(-\gamma-\ln(4\lambda\pi/3))/3+(1/2)=\mathrm{E}[\ln(R_2)]+(1/6)$
R_4	$(128/81)\pi^4\lambda^4 r_4^{11} \exp(-4\pi\lambda r_4^3/3)$	$(-\gamma-\ln(4\lambda\pi/3))/3+(11/18)=\mathrm{E}[\ln(R_3)]+(1/9)$
R_5	$(128/243)\pi^5\lambda^5 r_5^{14} \exp(-4\pi\lambda r_5^3/3)$	$(-\gamma-\ln(4\lambda\pi/3))/3+(50/72)=\mathrm{E}[\ln(R_4)]+(1/12)$
R_6	$(512/3645)\pi^6\lambda^6 r_6^{17} \exp(-4\pi\lambda r_6^3/3)$	$(-\gamma-\ln(4\lambda\pi/3))/3+(274/360)=\mathrm{E}[\ln(R_5)]+(1/15)$
R_7	$(1024/32805)\pi^7\lambda^7 r_7^{20} \exp(-4\pi\lambda r_7^3/3)$	$(-\gamma-\ln(4\lambda\pi/3))/3+(294/360)=\mathrm{E}[\ln(R_6)]+(1/18)$

In $\mathrm{Ex}(c\varepsilon^3)$, it is found that $c\varepsilon^3$ should be much smaller than one. Therefore, $\mathrm{Ex}(c\varepsilon^3)$ can be approximated by the following equation [22]:

$$\begin{aligned}\mathrm{Ex}(z) &= -\gamma-\ln(z)+\sum_{k=1}^{\infty}\frac{(-1)^{k+1}z^k}{k\cdot k!}\\ &\approx -\gamma-\ln(z) \quad \text{when} \quad z\ll 1\\ \Rightarrow \mathrm{Ex}(c\varepsilon^3) &\approx -\gamma-\ln(c\varepsilon^3). \end{aligned} \tag{9}$$

γ is the Euler-Mascheroni constant, which is equal to 0.5772. Through this approximation, we can identify the closed form of $E[\ln(R_1)]$, i.e.,

$$E\left[\ln(R_1)\right]=\left(-\gamma-\ln(4\pi\lambda/3)\right)/3. \tag{10}$$

Then, we apply the same approach to $E[\ln(R_n)]$. The closed forms of $E[\ln(R_n)]$ are listed in Table II for $n=1$ to 7. According to Table II, we conclude that $E[\ln(R_n)]$ can be estimated by the following equation for all $n\geq 2$:

$$E\left[\ln(R_n)\right]=E\left[\ln(R_1)\right]+\sum_{k=2}^{n}\frac{1}{3(k-1)}, \qquad n\geq 2. \tag{11}$$

This estimation will be verified by numerical simulation later.

III. FEMTO BASE STATION DENSITY ANALYSIS

In this section, we study the feasible femto BS densities in cellular network. Depending on interfering sources in the analysis model, we propose the following four scenarios: 1) the macro BS as the serving BS; 2) the macro BS as the dominant interference source; 3) the CSG femto BS as the dominant interference source to a non-CSG user; and 4) OSG femto BS network.

A. Macro BS as the Serving BS

In scenario 1, the user is served by the macro BS and surrounded by a group of interfering femto BSs. We assume that $P_{fn}=P_f$, $\delta_{fn}=\delta_f$, and $n=1,2,\ldots$. Based on [17], the SIR of the user can be simplified by the ratio of the received signal strength from the macro BS $(U_m(R_m))$ and U_1, i.e.,

Scenario 1

$$\begin{aligned}\mathrm{SIR}(R_m)&\approx U_m(R_m)-U_1\equiv \varsigma_a(R_m)\\ &=\left(P_m-\delta_m-10\eta_m\log_{10}(R_m)\right)\\ &\quad-\left(P_{f1}-\delta_{f1}-10\eta_f\log_{10}(R_1)\right).\end{aligned} \tag{12}$$

Here, P_m is the macro BS power, η_m is the path-loss exponent between the macro BS and the user, and R_1 is the distance between the user and the dominating interference source (the first nearest femto BS). The probability of outage events $\varsigma_a(R_m)<T_\varsigma$ should be limited by Pr_O (which is the maximum feasible outage probability of the cellular system), and T_ς is the minimum target SIR. The requirement is expressed as

$$\Pr\left(\varsigma_a(R_m)<T_\varsigma|R_m\right)<\mathrm{Pr}_O\,. \tag{13}$$

Theorem I: To satisfy the conditional outage probability $\Pr(\varsigma_a(R_m)<T_\varsigma|R_m)<\mathrm{Pr}_O$, the feasible femto BS density in scenario 1, i.e., λ^a, should follow the inequality given by

$$\begin{aligned}\lambda^a &< -3\ln(1-\mathrm{Pr}_O)\exp\left(-3T_\varsigma^a\right)/(4\pi)\\ T_\varsigma^a &= \ln(10)\left(T_\varsigma-(P_m-P_{f1})+(\delta_m-\delta_{f1})\right.\\ &\quad\left.+10\eta_m\log_{10}(R_m)\right)/(10\eta_f).\end{aligned} \tag{14}$$

Proof: It is clear that $\varsigma_a(R_m)$ is influenced by $\log_{10}(R_1)$. From (12), the outage event can be calculated by the following inequality:

$$\begin{aligned}\ln(R_1)<\ln(10)&\left(T_\varsigma-(P_m-P_{f1})+(\delta_m-\delta_{f1})\right.\\ &\left.+10\eta_m\log_{10}(R_m)\right)/(10\eta_f)\equiv T_\varsigma^a.\end{aligned} \tag{15}$$

By defining $Z_1\equiv\ln(R_1)$, the pdf of Z_1 is obtained through (5), i.e.,

$$\mathrm{Pr}_{Z_1}(z_1)=4\pi\lambda^a\exp\left(-4\pi\lambda^a\exp(3z_1)/3+3z_1\right). \tag{16}$$

In addition to $\Pr_{Z_1}(z_1)$, we can calculate the cumulative distribution function (cdf) through the integration of $\Pr_{Z_1}(z_1)$, i.e.,

$$\begin{aligned}\Pr_{Z_1}(z_1 < Z) &= \int_0^Z 4\pi\lambda^a \exp\left(-4\pi\lambda^a \exp(3z_1)/3 + 3z_1\right) dz_1 \\ &= \exp(-4\pi\lambda^a/3) - \exp\left(-4\pi\lambda^a \exp(3Z)/3\right) \\ &\approx 1 - \exp\left(-4\pi\lambda^a \exp(3Z)/3\right). \end{aligned} \quad (17)$$

Here, we let $\exp(-4\pi\lambda^a/3) \approx 1$ during the analysis of λ^a. The cdf is equivalent to the probability of "infeasibility" for a given λ^a when the threshold is Z. Finally, the upper bound of λ^a can be discovered through the cdf and $\Pr_O$, i.e.,

$$\begin{aligned}&\Pr\left(\varsigma_a(R_m) < T_\varsigma | R_m\right) \\ &\quad = \Pr\left(Z_1 < T_\varsigma^a | R_m\right) \\ &\quad \approx 1 - \exp\left(-4\pi\lambda^a \exp\left(3T_\varsigma^a\right)/3\right) < \Pr_O \\ &\quad => \lambda^a < -3\ln(1-\Pr_O)\exp\left(-3T_\varsigma^a\right)/(4\pi). \end{aligned} \quad (18)$$

B. Macro BS as the Dominant Interference Source

In scenario 2, we discuss the condition that the user is served by F_1 and that the macro BS is the dominant interference source. Without loss of generality, we assume that $E[U_k] > E[U_{k+1}], k \geq 1$. In this scenario, we cannot extend the results of [17] because the interfering nodes do not obey HPPP. In this scenario, the macro BS is the dominant interfering node and a threshold κ_D^b, which is the difference in signal strength (in decibels) between the interfering macro BS and the first strongest interfering femto BS F_2, is used to decide the macro BS as the dominant interference source.

Definition I [Scenario 2]: Based on the assumption that F_1 is the serving femto BS, the macro BS is the dominant interference source when

$$\begin{aligned}U_m(R_m) - E[U_2] > \kappa_D^b &=> (P_m - \delta_m - 10\eta_m \log_{10}(R_m)) \\ &\quad - (P_{f_2} - \delta_{f_2} 10\eta_f E\left[\log_{10}(R_2)\right]) > \kappa_D^b. \end{aligned} \quad (19)$$

From (19), we can have a loose bound, even without considering the serving femto BS performance. We can treat that as an upper bound for scenario 2 to be valid

$$\begin{aligned}&(10\eta_m \log_{10}(R_m) - (P_m - P_{f2}) \\ &\quad + (\delta_m - \delta_{f2}) + \kappa_D^b)/(10\eta_f) < E\left[\log_{10}(R_2)\right] \\ &\quad = \left(-\gamma - \ln(4\pi\lambda^b/3) + 1\right)/\left(3\ln(10)\right) \\ &\quad => \lambda^b < 3\exp\left(1 - C_D^b\right)/(4\pi) \\ &C_D^b = 3\ln(10)\left(10\eta_m \log_{10}(R_m) - (P_m - P_{f2})\right. \\ &\qquad \left. + (\delta_m - \delta_{f2}) + \kappa_D^b\right)/(10\eta_f) + \gamma. \end{aligned} \quad (20)$$

Here, λ^b is the feasible femto BS density in scenario 2. To ensure that the conditional outage probability in scenario 2, i.e., $\Pr(\varsigma_b(R_m) < T_\varsigma | R_m)$, is lower than $\Pr_O$, we can calculate the condition for λ^b, i.e.,

Scenario 2

$$\begin{aligned}\text{SIR}(R_m) &\approx U_1 - U_m(R_m) \equiv \varsigma_b(R_m) \\ &= (P_{f1} - \delta_{f1} - 10\eta_f \log_{10}(R_1)) \\ &\quad - (P_m - \delta_m - 10\eta_m \log_{10}(R_m)). \end{aligned} \quad (21)$$

Therefore, λ^b should follow Theorem II.

Theorem II: To guarantee that the conditional outage probability can meet the requirement of $\Pr(\varsigma_b(R_m) < T_\varsigma | R_m) < \Pr_O$, the feasible femto BS density in scenario 2 should follow, i.e.,

$$\begin{aligned}&\lambda^b > 3\ln\left(\Pr_O^{-1}\right)\exp\left(-3T_\varsigma^b\right)/(4\pi) \\ &T_\varsigma^b = \ln(10)\left(-T_\varsigma - (P_m - P_{f1}) + (\delta_m - \delta_{f1})\right. \\ &\qquad \left. + 10\eta_m \log_{10}(R_m)\right)/(10\eta_f) \end{aligned} \quad (22)$$

and the prerequirement of having the macro BS as the dominating interference source [derived from (20)], i.e.,

$$\begin{aligned}&\lambda^b < 3\exp\left(1 - C_D^b\right)/(4\pi) \\ &C_D^b = 3\ln(10)\left(10\eta_m \log_{10}(R_m) - (P_m - P_{f2})\right. \\ &\qquad \left. + (\delta_m - \delta_{f2}) + \kappa_D^b\right)/(10\eta_f) + \gamma. \end{aligned} \quad (23)$$

Proof: In the following, we prove only the inequality of (22):

$$\begin{aligned}&(P_{f_1} - \delta_{f1} - 10\eta_f \log_{10}(R_1)) \\ &\quad - (P_m - \delta_m - 10\eta_m \log_{10}(R_m)) < T_\varsigma \\ &\quad => \ln(R_1) > \ln(10) \\ &\qquad \times \left(-T_\varsigma - (P_m - P_{f1}) + (\delta_m - \delta_{f1})\right. \\ &\qquad \left. + 10\eta_m \log_{10}(R_m)\right)/(10\eta_f) \equiv T_\varsigma^b. \end{aligned} \quad (24)$$

In (18), we have obtained the closed form of $\Pr(Z_1 < T_\varsigma^a | R_m)$, which can also be applied in the inequality $\Pr(U_1 - U_m(R_m) < T_\varsigma | R_m)$ to calculate the requirement of λ^b, i.e.,

$$\begin{aligned}&\Pr\left(U_1 - U_m(R_m) < T_\varsigma | R_m\right) \\ &\quad = \Pr_{Z_1}\left(z_1 > T_\varsigma^b \middle| R_m\right) \\ &\quad \approx \exp\left(-4\pi\lambda^b \exp\left(3T_\varsigma^b\right)/3\right) < \Pr_O \\ &\quad => \lambda^b > 3\ln\left(\Pr_O^{-1}\right)\exp\left(-3T_\varsigma^b\right)/(4\pi). \end{aligned} \quad (25)$$

Based on Theorem II, there are feasible values of λ^b in scenario 2 when it is located in the range defined in Theorem II. Note that both scenario 2 and its feasible λ^b exist when

$$C_D^b < 1 + 3T_\varsigma^b - \ln\left(\ln(\Pr_O^{-1})\right). \quad (26)$$

C. CSG Femto BS as the Dominant Interference Source to a Non-CSG User

In scenario 3, we concentrate on the interference between two different femto BS networks, i.e., the OSG femto BS network and the CSG femto BS network. Both networks are uniformly distributed around a non-CSG user, where $F_{n,O}$ and $F_{n,C}$ are the nth nearest OSG and CSG femto BSs, respectively. The transmission powers and path-loss constants of $\{F_{n,O}, F_{n,C}\}$ are $\{P_{fn,O}, P_{fn,C}\}$ and $\{\delta_{fn,O}, \delta_{fn,C}\}$, respectively. The densities of the OSG and CSG femto BS networks are given by $\{\lambda_O^C, \lambda_C^C\}$. In this scenario, we consider the situation that interference is dominated by $F_{1,C}$ when the user is served by $F_{1,O}$. Therefore, we assume $E[U_{1,C}] > \text{MAX}\{E[U_{2,O}], E[U_{2,C}]\}$ by giving the Definition II.

Definition II [Scenario 3]: Based on the assumption that $F_{1,O}$ is the serving BS and that $P_{f2,O} \geq P_{f3,O} \geq \cdots$, $P_{f2,C} \geq P_{f3,C} \geq \cdots$, $\delta_{f2,O} \leq \delta_{f3,O} \leq \cdots$, and $\delta_{f2,C} \leq \delta_{f3,C} \leq \cdots$, $F_{1,C}$ is the dominant interference source when

$$E[U_{1,C}] - \text{MAX}\{E[U_{2,O}], E[U_{2,C}]\} > \kappa_D^C.$$

$$\begin{cases} E[U_{1,C}] = P_{f1,C} - \delta_{f1,C} - 10\eta_f E\left[\log_{10}(R_{1,C})\right] \\ E[U_{2,C}] = P_{f2,C} - \delta_{f2,C} - 10\eta_f E\left[\log_{10}(R_{2,C})\right] \\ E[U_{2,O}] = P_{f2,O} - \delta_{f2,O} - 10\eta_f E\left[\log_{10}(R_{2,O})\right] \end{cases} \quad (27)$$

where $\{U_{n,O}, U_{n,C}\}$ are the received signal strengths from $\{F_{n,O}, F_{n,C}\}$, and $\{R_{n,O}, R_{n,C}\}$ are the distances from $\{F_{n,O}, F_{n,C}\}$ to the non-CSG user. In addition to (27), we still need to estimate the requirements of $(\lambda_O^C, \lambda_C^C)$ to ensure that SIR $> T_\varsigma$, i.e.,

Scenario 3

$$\begin{aligned} \text{SIR} &\approx U_{1,O} - U_{1,C} \equiv \varsigma_c \\ &= (P_{f1,O} - \delta_{f1,O} - 10\eta_f \log_{10}(R_{1,O})) \\ &\quad - (P_{f1,C} - \delta_{f1,C} - 10\eta_f \log_{10}(R_{1,C})). \end{aligned} \quad (28)$$

However, the closed form of ς_c is not obvious because both $R_{1,O}$ and $R_{1,C}$ are random variables. To obtain a clear view of the influence of $(\lambda_O^C, \lambda_C^C)$, we assume that the outage probability can be controlled when $E[\varsigma_c] > \kappa_T^C$. We then propose Theorem III for feasible values of $(\lambda_O^C, \lambda_C^C)$.

Theorem III: To guarantee $E[\varsigma_c] > \kappa_T^C$ in scenario 3, the feasible $(\lambda_C^C, \lambda_O^C)$ should follow as

$$\begin{aligned} &\lambda_C^C < \lambda_O^C \exp\left(-C_T^C\right) \\ &C_T^C = 3\ln(10)\left(\kappa_T^C + (P_{f1,C} - P_{f1,O}) \right. \\ &\qquad \left. - (\delta_{f1,C} - \delta_{f1,O})\right)/(10\eta_f) \end{aligned} \quad (29)$$

under the prerequirements of

$$\begin{aligned} &\lambda_O^C \exp\left(X_2^C\right) < \lambda_C^C < \lambda_O^C \exp\left(X_1^C\right) \\ &X_1^C = 3\ln(10)\left((P_{f2,O} - P_{f2,C}) - (\delta_{f2,O} - \delta_{f2,C})\right)/(10\eta_f) \\ &X_2^C = 3\ln(10)\left(\kappa_D^C - (P_{f1,C} - P_{f2,O}) \right. \\ &\qquad \left. + (\delta_{f1,C} - \delta_{f2,O})\right)/(10\eta_f) - 1 \end{aligned} \quad (30)$$

or

$$\begin{cases} \lambda_C^C > \lambda_O^C \exp\left(X_1^C\right) \\ (P_{f1,C} - P_{f2,C}) - (\delta_{f1,C} - \delta_{f2,C}) + 10\eta_f / \left(3\ln(10)\right) > \kappa_D^C. \end{cases} \quad (31)$$

Proof:

1) Replacing (28) with the closed forms of $E[\ln(R_{1,C})]$ and $E[\ln(R_{1,O})]$, we obtain

$$\begin{aligned} &E\left[\ln(R_{1,C})\right] - E\left[\ln(R_{1,O})\right] \\ &\quad > \ln(10)\left(\kappa_T^C + (P_{f1,C} - P_{f1,O}) - (\delta_{f1,C} - \delta_{f1,O})\right)/(10\eta_f) \\ &\quad => \lambda_C^C < \lambda_O^C \exp\left(-C_T^C\right) \end{aligned}$$

$$\begin{aligned} C_T^C = 3\ln(10)&\left(\kappa_T^C + (P_{f1,C} - P_{f1,O}) \right. \\ &\left. - (\delta_{f1,C} - \delta_{f1,O})\right)/(10\eta_f). \end{aligned} \quad (32)$$

2) We examine two cases to analyze the inequality in (27).

Case 1: $E[U_{2,O}] > E[U_{2,C}]$*:*

(a) If $E[U_{2,O}] > E[U_{2,C}]$, then $(\lambda_O^C, \lambda_C^C)$ should follow as

$$\lambda_C^C < \lambda_O^C \exp\left(X_1^C\right)$$

$$X_1^C = 3\ln(10)\left((P_{f2,O} - P_{f2,C}) - (\delta_{f2,O} - \delta_{f2,C})\right)/(10\eta_f). \quad (33)$$

(b) If $E[U_{2,O}] > E[U_{2,C}]$, (27) is equivalent to $E[U_{1,C}] - E[U_{2,O}] > \kappa_D^C$. $(\lambda_O^C, \lambda_C^C)$ should then follow as

$$\begin{aligned} &\lambda_C^C > \lambda_O^C \exp\left(X_2^C\right) \\ &X_2^C = 3\ln(10)\big(\kappa_D^C - (P_{f1,C} - P_{f2,O}) \\ &\qquad + (\delta_{f1,C} - \delta_{f2,O})\big)/(10\eta_f) - 1. \end{aligned} \quad (34)$$

(c) From (a) and (b), we can identify the prerequirement for scenario 3 when $E[U_{2,O}] > E[U_{2,C}]$.

Case 2: $E[U_{2,C}] > E[U_{2,O}]$*:*

(a) If $E[U_{2,C}] > E[U_{2,O}]$, then $(\lambda_O^C, \lambda_C^C)$ should follow as

$$\lambda_C^C > \lambda_O^C \exp\left(X_1^C\right). \quad (35)$$

(b) If $E[U_{2,C}] > E[U_{2,O}]$, (27) is equivalent to $E[U_{1,C}] - E[U_{2,C}] > \kappa_D^C$. $(\lambda_O^C, \lambda_C^C)$ should then follow as

$$(P_{f1,C} - P_{f2,C}) - (\delta_{f1,C} - \delta_{f2,C}) + 10\eta_f / \left(3\ln(10)\right) > \kappa_D^C. \quad (36)$$

(c) From (a) and (b), we can identify the prerequirement for scenario 3 when $E[U_{2,C}] > E[U_{2,O}]$.

Therefore, given λ_O^C, the feasible λ_C^C can be found by Theorem III. In the Appendix, we explain how to obtain κ_T^C.

D. OSG Femto BS Network

In scenario 4, we discuss the condition that the user is surrounded by an OSG femto BS network. Here, we assume that F_1 is the serving femto BS and F_2 is the dominant interference

TABLE III
NOTATIONS IN THE FEMTO BS NETWORK ANALYSIS MODEL

Notation	Definition	Value
P_m	Radiation power of macro BS	46 dBm
$\{P_{fn}, P_{fn,C}, P_{fn,O}\}$	Radiation power of $\{F_n, F_{n,O}, F_{n,C}\}$.	20 dBm
R_m	Distance from the macro BS to the user	50–700 m
R_n n = 1 ~ N	Distance from F_n to the user	$\varepsilon \le R_n$
δ_m	Path loss constant of macro BS	50 dB
$\{\delta_{fn}, \delta_{fn,C}, \delta_{fn,O}\}$	Path loss constant of $\{F_n, F_{n,C}, F_{n,O}\}$	35–65 dB
ε	Minimum distance of R_n	1 m
η_m	Path loss exponent of macro BS path	3
η_f	Path loss exponent of femto BS path	3.5
γ	Euler-Mascheroni constant	0.5772
$\Pr_O$	System requirement of the upper bound of outage probability	0.1
T_ς	SIR threshold of the outage event	3 dB
κ_D^b	Dominating threshold of scenario 2	12.11 dB
κ_T^C	Outage threshold of scenario 3	14.65 dB
κ_D^C	Dominating threshold of scenario 3	10 dB
κ_D^d	Dominating threshold of scenario 4 to ignore the macro BS	18 dB

source. We assume that the outage probability can be controlled when $E[\text{SIR}] > \kappa_T^d$, i.e.,

Scenario 4

$$E[\text{SIR}] \approx E[U_1] - E[U_2] \equiv \bar{\varsigma}_d > \kappa_T^d$$
$$\Rightarrow (P_{f1} - \delta_{f1} - 10\eta_f E[\log_{10}(R_1)]) - (P_{f2} - \delta_{f2} - 10\eta_f E[\log_{10}(R_2)]) > \kappa_T^d. \quad (37)$$

By replacing $E[\log_{10}(R_1)]$ and $E[\log_{10}(R_2)]$ with the closed forms in Table II, we obtain the following inequality:

$$(P_{f1} - P_{f2}) - (\delta_{f1} - \delta_{f2}) > \kappa_T^d - 10\eta_f / (3\ln(10)). \quad (38)$$

It is clear that (38) is unrelated with the density of femto BS networks. In the next section, we will verify the proposed algorithms through simulations.

IV. SIMULATIONS

In this section, we verify the aforementioned theorems through numerical simulations. In the simulations, the parameters are set according to Table III. Before verifying Theorems I–III, we first verify the closed forms of estimated $E[\ln(R_n)]$ in (11). In Fig. 2, we compare the numerical simulation of $E[U_n]$ and the closed form of $E[U_n]$ [by using (11)], which are represented by $E[U_n]$(Num) and $E[U_n]$(Est), respectively. From Fig. 2, it is clear that $E[U_n]$(Num) and $E[U_n]$(Est) match different femto BS densities.

In the following numerical simulations, to accommodate the most influential femto BSs, we will select the ten nearest femto BSs to represent the interference impacts from the femto BS network, where the signal strength difference between the first nearest femto BS and the tenth nearest femto BS is about 15 dB,

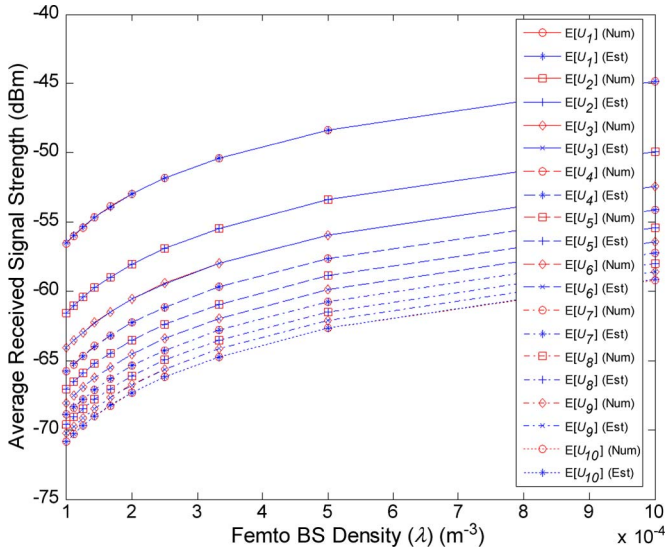

Fig. 2. Comparison of $E[U_n]$(Num) and $E[U_n]$(Est), and $\delta_{f1} = \delta_{f2} = \cdots = 40$ dB.

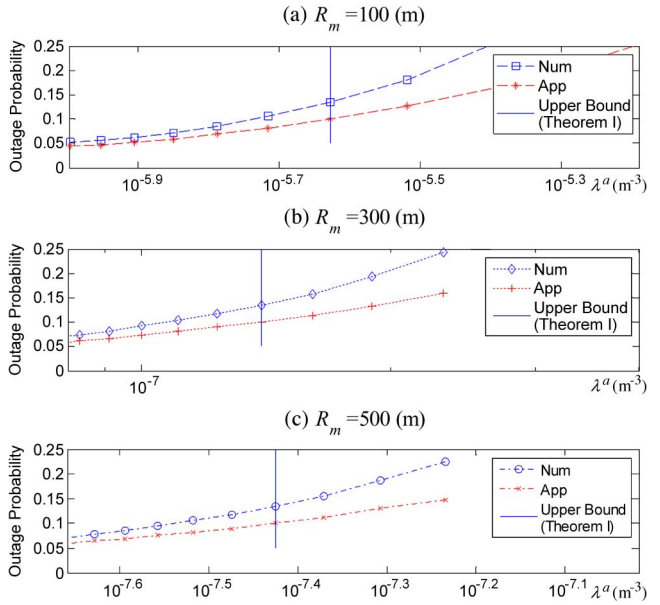

Fig. 3. Outage probability estimated with λ^a in Theorem I, where $\delta_{f1} = \delta_{f2} = \cdots = 40$ dB. Here, we assume R_m is equal to 100 m, 300 m, and 500 m in the (a), (b), and (c), respectively.

as also shown in Fig. 2. To verify the theorems, we will compare the numerical simulations (Num) with the approximation (App) based on the dominating interference source only, and the theorem bounds are calculated for operating at 10% outage probability.

For Theorem I, considering different R_m's (the distance between the user and the macro BS), Fig. 3 plots the feasible femto BS density λ^a with outage probability of Num and App. As shown, when operated at a low outage probability ($\sim$5%), the approximation in feasible femto BS density, based on the "nearest femto BS only," has good representation of overall interference impacts. In addition, as expected, when R_m increases, the feasible femto BS density decreases.

In Fig. 4, with various R_m, we will show the changes in feasible femto BS densities λ^a and λ^b of Theorems I and II, respectively. Here, instead of considering a fixed path-loss

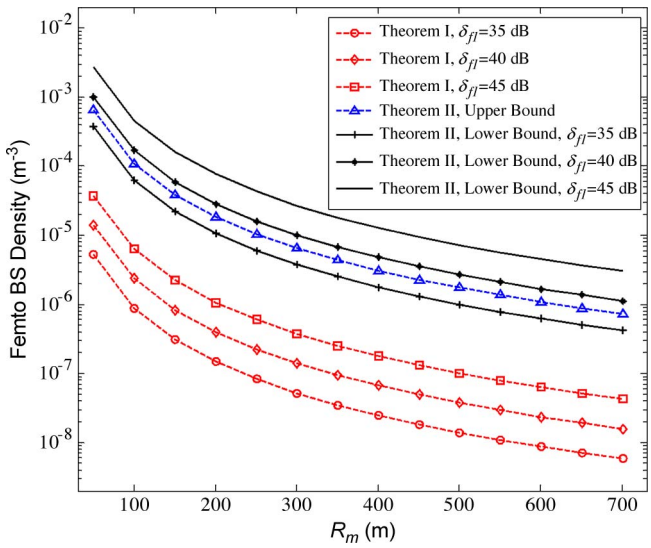

Fig. 4. Feasible regions of λ^a and λ^b. Here, we assume that $\delta_{f2} = \delta_{f3} = \cdots = 55$ dB and adjust δ_{f1} from 35 to 45 dB.

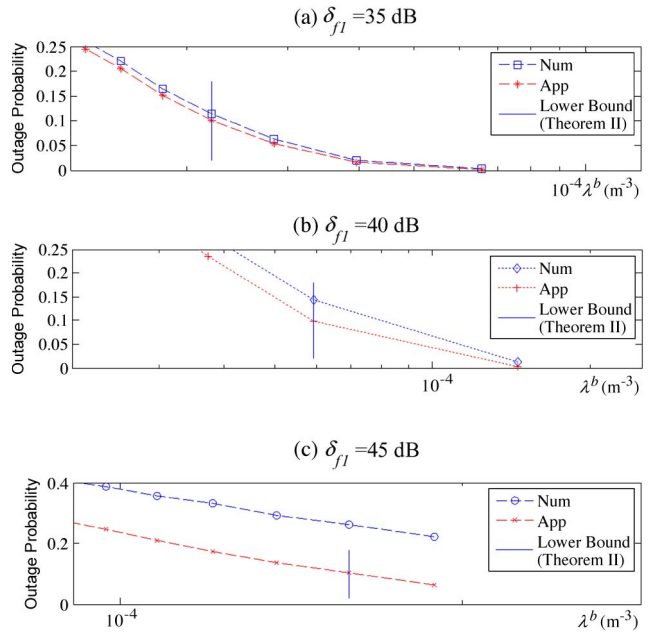

Fig. 5. Outage probability when λ^b is located near the lower bound estimated from Theorem II, where $\delta_{f2} = \delta_{f3} = \cdots = 55$ dB and $R_m = 150$ m. Here, we assume δ_{f1} is equal to 35 dB, 40 dB, and 45 dB in the (a), (b), and (c), respectively.

constant of 40 dB of all in Fig. 3, we adjust δ_{f1} to 35, 40, and 45 dB, and other δ_{fn}'s are fixed at 55 dB. From Fig. 4, for either scenarios 1 or 2, the bounds of feasible femto BS density more rapidly drop when R_m is in the range of 200 m, and then, the tendency slows down when $R_m > 200$ m. For scenario 1, the nearest femto BS is the dominating interference source, and the lower path-loss constant will decrease the upper bound of the feasible femto BS density. On the contrary, for scenario 2, the nearest femto BS is the serving BS, and the lower path-loss constant will increase the range of feasible femto BS densities. Furthermore, to meet the scenario criterion of having the macro BS as the dominating interference source (which is calculated as a loose upper bound), the path-loss constant of the nearest femto BS should below 40 dB (∼38 dB).

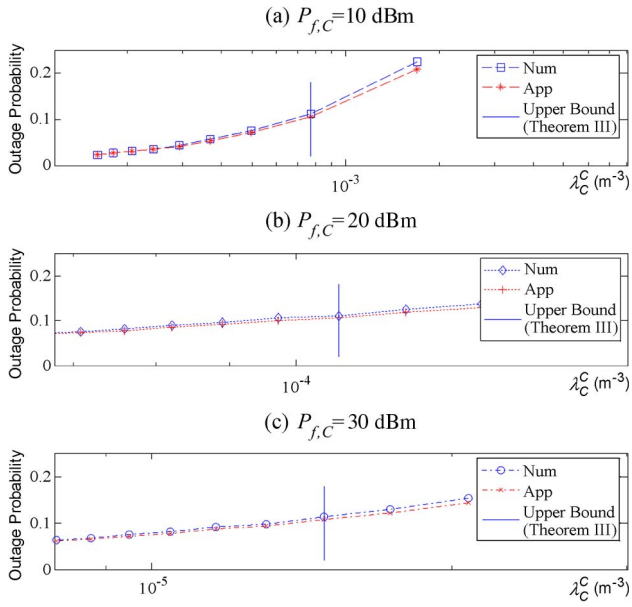

Fig. 6. Outage probability when λ_C^C is located near the upper bound estimated from Theorem III. Here, $\delta_{f1,O} = 40$ dB, $\delta_{f1,C} = 55$ dB, $\delta_{f2,O} = \delta_{f3,O} = \cdots = 65$ dB, $\delta_{f2,C} = \delta_{f3,C} = \cdots = 65$ dB, and $\lambda_O^C = 10^{-4}$ m^{-3}. We assume $P_{f,c}$ is equal to 10 dBm, 20 dBm, and 30 dBm in the (a), (b), and (c), respectively.

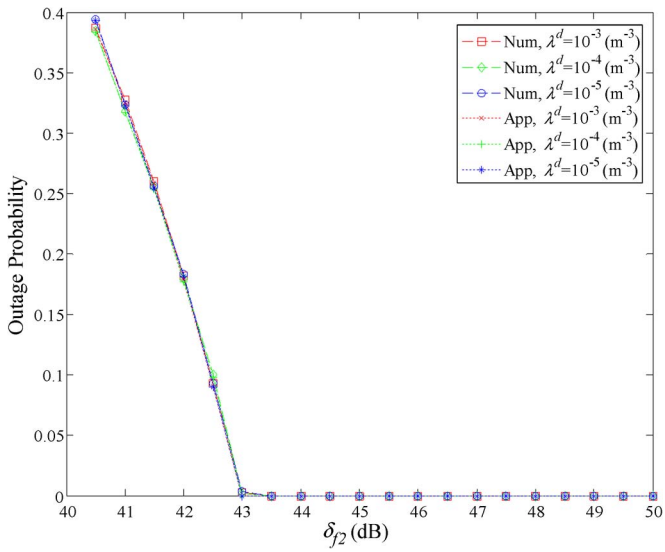

Fig. 7. Outage probability of scenario 4. Here, $\delta_{f1} = 40$ dB, $\delta_{f3} = \cdots = 65$ dB, and $\delta_{f2} = 41-50$ dB. It is clear that the outage probability is unrelated to λ^d.

In Fig. 5, with a fixed $R_m = 150$ m, we evaluate the feasible femto BS density with outage probability for Num and App. From Fig. 5, it is clear that, for the $\delta_{f1} = 35$ dB plot, the App and Num curves match well. For other two ($\delta_{f1} = 40$ dB and 45 dB), since, from Fig. 4, the associated lower bounds exceed the upper bound, which violates the assumption of having the macro BS as the dominating interference source, the App and Num departs from each other.

If considering femto BS as the dominating interference source, from Fig. 6, the App and Num curves match well in various operating outage probabilities in the scenario 3, where the nearest CSG femto BS is the dominant interference node to the non-CSG user. In Fig. 7, we verify our observation of scenario 4, where both the serving femto BS and the dominating

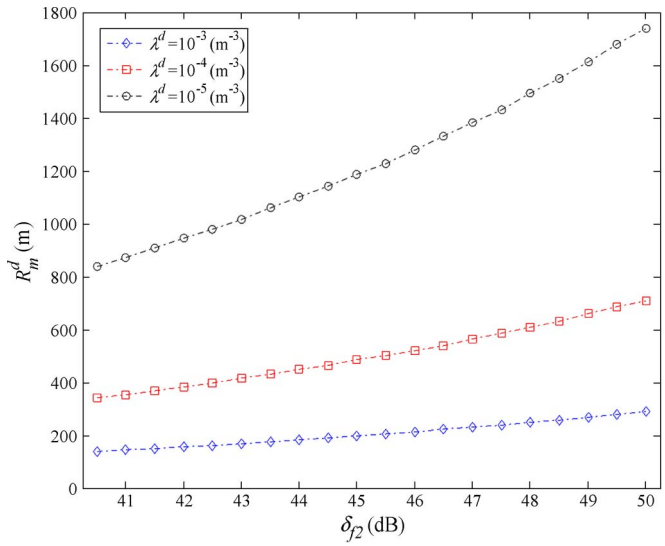

Fig. 8. Curves of R_m^d under different δ_{f2}'s and λ^d's. Here, $\delta_{f1} = 40$ dB, $\delta_{f3} = \cdots = 65$ dB, and $\delta_{f2} = 41-50$ dB.

interference node are from the same OSG femto BS network. By adjusting λ^d in Fig. 7, we found that the outage probability is unrelated to λ^d, and this result coincides with our analysis in scenario 4.

In scenario 4, to ignore the interference from the macro BS, the minimum distance R_m^d between the user and macro BS is plotted in Fig. 8. Here, we assume that the interference from the macro BS can be ignored when $E[U_2] - U_m(R_m) > \kappa_D^d$. κ_D^d is obtained through numerical simulation, and R_m^d is the minimum value to fulfill the inequality. In Fig. 8, we consider different femto BS densities and various path-loss constants of the dominating interference femto BS F_2. As expected, the minimum distance increases with the decrease in femto BS density. When the femto BS density is higher, the minimum distance becomes less sensitive to the change of path-loss constant from the dominating interference femto BS.

V. Discussion

Considering four different deployment scenarios, we have identified closed-form solutions to analyze related deployment performance of femto BS networks. The results can provide a reference for the deployment of femto BS networks.

First, Theorems I and II, corresponding to scenarios 1 and 2, respectively, provide the average user performance in a mixed macro BS and femto BS network and the feasible femto BS density when the macro BS is either the serving BS or dominating interference source. The resulting feasible femto BS density can be used as design criteria for resource allocation. For example, when the femto BS density exceeds a threshold, the original cochannel resource allocations might need to be switched to orthogonal channel allocations to avoid further degradation of the system performance due to the excessive interference.

The same concept applies to the conditions of a mixed CSG and OSG femto BS network or a complete OSG femto BS network. Based on the observation in the scenarios 3 and 4, the feasible femto BS density can be calculated. From that, the operator can use the reference threshold to activate the hybrid access of CSG and OSG or again to consider the orthogonal channel allocation scheme to mitigate the interference problems.

In conclusion, the proposed model provides simple approximation of user performance in four different deployment scenarios. Operators can then quickly verify the overall performance and decide proper resource allocation schemes to maintain the quality of service of their networks.

VI. Conclusion

In this paper, combining stochastic geometry for femto BS deployment and low outage probability criterion for cellular networks, we have been able to derive a closed-form solution of a feasible femto BS density in 3-D space by assuming the existence of a dominating interference source. To generalize the deployment scenarios, we have considered four different scenarios: 1) the macro BS as the serving BS; 2) the macro BS as the dominant interference source; 3) the CSG femto BS as the dominant interference source to a non-CSG user; and 4) the OSG femto BS network. Results show that the approximation from the assumption of dominating interfering source is actually a good representation of user performance in the aforementioned four different scenarios, which can be used to provide a quick evaluation of the limit in femto BS density under the low outage probability criterion.

Appendix

Here, we provide a method to estimate the appropriate κ_T^C in the Theorem III. We start the analysis from $\Pr_{Z_1}(z_1)$, i.e.,

$$\Pr_{Z_1}(z_1) = 4\pi\lambda \cdot \exp(-4\pi\lambda \exp(3z_1)/3 + 3z_1). \quad \text{(A.1)}$$

From (A.1), it is clear that $\exp(3z_1)$ dominates the left tail of $\Pr_{Z_1}(z_1)$ and that $\exp(-4\pi\lambda\exp(3z_1)/3)$ dominates the right tail. We approximate the left tail of $\Pr_{Z_1}(z_1)$ by the following equation:

$$\begin{aligned}&\text{Left tail of } \Pr_{Z_1}(z_1)\\ &\quad\approx 4\pi\lambda\exp(3Z_1)\\ &\quad\approx \frac{1}{\sqrt{2\pi C_{Z_1}^2}}\exp(3Z_1)\exp\left(-Z_1^2/\left(2C_{Z_1}^2\right)\right)\\ &C_{Z_1}^2 \equiv (32\pi^3\lambda^2)^{-1} => -Z_1^2/\left(2C_{Z_1}^2\right) \approx 0. \quad \text{(A.2)}\end{aligned}$$

$C_{Z_1}^2$ is very close to zero, and the range of Z_1 is small.

Therefore, the attached exponential term does not affect the pdf in an obvious way. Thus, we can further extend the approximation as

$$\begin{aligned}&\text{Left tail of } \Pr_{Z_1}(z_1)\\ &\approx \frac{1}{\sqrt{2\pi C_{Z_1}^2}}\cdot\exp(3Z_1)\exp\left(\frac{-Z_1^2}{2C_{Z_1}^2}\right)\\ &\quad\times\exp\left(\frac{-9C_{Z_1}^2}{2}\right)\exp\left(\frac{9C_{Z_1}^2}{2}\right)\\ &= \frac{\exp\left(9C_{Z_1}^2/2\right)}{\sqrt{2\pi C_{Z_1}^2}}\exp\left(-\left(Z_1-3C_{Z_1}^2\right)^2/\left(2C_{Z_1}^2\right)\right)\\ &= \exp\left(9C_{Z_1}^2/2\right)\Pr(N_{Z_1}),\quad N_{Z_1}\sim N\left(3C_{Z_1}^2, C_{Z_1}^2\right).\end{aligned} \quad \text{(A.3)}$$

$$\mathrm{var}(Z_1) = \sigma_{Z_1}^2 = E\left[\ln^2(R_1)\right] - E\left[\ln(R_1)\right]^2$$

$$E\left[\ln^2(R_1)\right] = \int_{\varepsilon}^{\infty} 4\pi\lambda r_1^2 \ln^2(r_1)\exp(-4\pi\lambda r_1^3/3)dr_1.$$

$$\int \ln^2(x)x^2\exp(-cx^3)dx$$

$$= \frac{x^3}{3}\left(\frac{2\cdot {}_3F_3(1,1,1;2,2,2;-cx^3)}{9} - \frac{\ln(x)\left((3\exp(-cx^3)-3)\ln(x)+2\left(\ln(cx^3)+\gamma\right)+2\Gamma(0,cx^3)\right)}{3cx^3}\right) \quad \text{(A.5)}$$

Based on observations, the left tails of $\ln(R_{1,C})$ and $\ln(R_{1,O})$ are very similar to that of normal distribution. Therefore, we expect the left tail of ς_C to be similar to that of normal distribution because $\exp(3z_1)$ will also dominate the left term during the convolution process. We propose to use the cdf of normal distribution to find κ_T^C, i.e.,

$$\Pr(\varsigma_C < T_\varsigma) < \frac{1}{2}\left(1+\mathrm{erf}\left(\frac{T_\varsigma - \bar{\varsigma}_C}{\sqrt{2}\sigma_C}\right)\right) < \Pr_O$$

$$=> \bar{\varsigma}_C > T_\varsigma - \sqrt{2}\sigma_C \mathrm{erf}^{-1}(2\Pr_O - 1) \equiv \kappa_T^C$$

$$\sigma_C^2 = \mathrm{Var}(U_{1,O}) + \mathrm{Var}(U_{1,C}). \quad \text{(A.4)}$$

In other words, we can approximate the probability of "infeasibility" of a given λ_C^C by utilizing the cdf of normal distribution. In (A.4), it is observed that κ_T^C also depends on σ_C, which is determined by the variance of Z_1, $\mathrm{var}(Z_1)$. $\mathrm{var}(Z_1)$ can be represented by (A.5), shown at the top of the page.

The integration in (A.5) is also obtained from [21]. Here, σ_{Z_1} is the standard deviation of Z_1, $\Gamma(0, cx^3)$ is the incomplete Gamma function, and ${}_3F_3(1, 1, 1; 2, 2, 2; -cx^3)$ is the generalized hypergeometric function. It is difficult to obtain a closed form for the integration. However, through our numerical simulations, we found that σ_{Z_1} remains stable when we adjust λ across a wide range of values. Based on this observation, we assume $\mathrm{Var}(U_{1,O}) = \mathrm{Var}(U_{1,C}) = \mathrm{Var}(U_1)$ because both $\mathrm{Var}(U_{1,O})$ and $\mathrm{Var}(U_{1,C})$ would also be stable with the change in the femto BS density. Therefore, we assume that $\sigma_C^2 = 2\mathrm{Var}(U_1)$ in the estimation of κ_T^C. $\mathrm{Var}(U_1)$ can be estimated by numerical simulation.

REFERENCES

[1] IEEE Std. P802.16m/D6, May 2010.

[2] *3rd Generation Partnership Project; Technical Specification Group Radio Access Networks; 3G Home NodeB Study Item Technical Rep. 3GPP TR 25.820 V8.2.0*, Sep. 2008.

[3] V. Chandrasekhar, J. G. Andrews, and A. Gatherer, "Femtocell networks: A survey," *IEEE Commun. Mag.*, vol. 46, no. 9, pp. 59–67, Sep. 2008.

[4] S. P. Yeh, S. Talwar, S. C. Lee, and H. Kim, "WiMAX femtocells: A perspective on network architecture, capacity, and coverage," *IEEE Commun. Mag.*, vol. 46, no. 10, pp. 58–65, Oct. 2008.

[5] N. Arulselvan, V. Ramachandran, S. Kalyanasundaram, and G. Han, "Distributed power control mechanisms for HSDPA femtocells," in *Proc. IEEE 69th Vehicular Technol. Conf.*, Barcelona, Spain, Apr. 26–29, 2009, pp. 1–5.

[6] V. Chandrasekhar, J. G. Andrews, T. Muharemovic, Z. Shen, and A. Gatherer, "Power control in two-tier femtocell networks," *IEEE Trans. Wireless Commun.*, vol. 8, no. 8, pp. 4316–4328, Oct. 2009.

[7] H. Claussen, L. T. W. Ho, and L. G. Samuel, "Self-optimization of coverage for femtocell deployments," in *Proc. IEEE Wireless Telecommun. Symp.*, Pomona, CA, Apr. 24–26, 2008, pp. 278–285.

[8] L. G. U. Garcia, K. I. Pedersen, and P. E. Mogensen, "Autonomous component carrier selection: Interference management in local area environments for LTE-advanced," *IEEE Commun. Mag.*, vol. 47, no. 9, pp. 110–116, Sep. 2009.

[9] D. Lopez-Perez, A. Ladanyi, A. Juttner, and J. Zhang, "OFDMA femtocells: A self-organizing approach for frequency assignment," in *Proc. IEEE 20th Int. Symp. Pers., Indoor Mobile Radio Commun.*, Tokyo, Japan, Sep. 13–16, 2009, pp. 2202–2207.

[10] K. Sundaresan and S. Rangarajan, "Efficient resource management in OFDMA femto cells," in *Proc. 10th ACM Int. Symp. Mobile Ad Hoc Netw. Comput. ACM MobiHoc*, New Orleans, LA, May 18–21, 2009, pp. 33–42.

[11] B. D. Ripley, *Spatial Statistics*. Hoboken, NJ: Wiley, Aug. 2004, ch. 7.

[12] G. J. G. Upton and B. Fingleton, *Spatial Data Analysis by Example: Point Pattern and Quantitative Data*. Hoboken, NJ: Wiley, Apr. 1985.

[13] M. Haenggi, J. G. Andrews, F. Baccelli, O. Dousse, and M. Franceschetti, "Stochastic geometry and random graphs for the analysis and design of wireless networks," *IEEE J. Sel. Areas Commun.*, vol. 27, no. 7, pp. 1029–1046, Sep. 2009.

[14] J. G. Andrews, R. K. Ganti, M. Haenggi, N. Jindal, and S. Weber, "A primer on spatial modeling and analysis in wireless networks," *IEEE Commun. Mag.*, vol. 48, no. 11, pp. 156–163, Nov. 2010.

[15] V. Chandrasekhar and J. G. Andrews, "Spectrum allocation in tiered cellular networks," *IEEE Trans. Commun.*, vol. 57, no. 10, pp. 3059–3068, Oct. 2009.

[16] S. Weber and J. G. Andrews, "A stochastic geometry approach to wideband ad hoc networks with channel variations," in *Proc. IEEE 4th Int. Symp. Model. Optim. Mobile, Ad Hoc Wireless Netw.*, Boston, MA, Apr. 3–6, 2006, pp. 1–6.

[17] V. Mordachev and S. Loyka, "On node density—Outage probability tradeoff in wireless networks," *IEEE J. Sel. Areas Commun.*, vol. 27, no. 7, pp. 1120–1131, Sep. 2009.

[18] "Simulation assumptions and parameters for FDD HeNB RF requirements," R4-092042, 3GPP TSG RAN WG4 (Radio) Meeting #51, San Francisco, CA2009, May 4–8.

[19] M. Haenggi, "On distances in uniformly random networks," *IEEE Trans. Inf. Theory*, vol. 51, no. 10, pp. 3584–3586, Oct. 2005.

[20] G. L. Stüber, *Principles of Mobile Communication*, 2nd ed. Norwell, MA: Kluwer, 2001.

[21] Wolfram Mathematica Online Integrator. [Online]. Available: http://integrals.wolfram.com/index.jsp

[22] M. Abramowitz and I. A. Stegun, *Handbook of Mathematical Functions: With Formulas, Graphs, and Mathematical Tables*. New York: Dover, Jun. 1974, pp. 228–229.

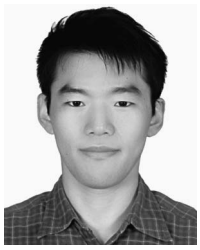

YungLan Tseng received the B.E. and M.E. degrees in 2003 and 2006, respectively, from National Chiao Tung University, HsinChu, Taiwan, where he is currently working toward the Ph.D. degree.

From 2006 to 2007, he was a Communication Officer with the R.O.C. Air Force. Since 2008, he has been a Research Assistant with the Institute for Information Industry, Taipei, Taiwan. His current research interests include cross-layer radio resource management in next-generation mobile wireless systems, femto base station networks, and machine type communications.

ChingYao Huang (M'08) received the B.S. degree in physics from National Taiwan University, Taipei, Taiwan, in 1987 and the Master and Ph.D. degrees in electrical and computer engineering from New Jersey Institute of Technology (NJIT), Newark, and Rutgers University, the State University of New Jersey, New Brunswick, in 1991 and 1996, respectively.

He joined AT&T, Whippany, NJ, and then Lucent Technologies in 1996 as a Member of Technical Staff. In 2001 and 2002, he was an Adjunct Professor with Rutgers University and NJIT. In 2002, he joined the Department of Electronics Engineering, National Chiao Tung University, HsinChu, Taiwan, where he is currently an Associate Professor and the Director of the Technology Licensing Office and Incubation Center. He has served as Editor for the *ACM Journal of Wireless Networks* and *Recent Patents on Electrical Engineering*. He has published more than 60 technical memorandums, journal papers, and conference proceeding papers. He is the holder of 16 patents. His research interests include wireless medium access controls for cellular, wireless body area networks, and wireless machine-to-machine communications.

Dr. Huang was the Technical Chair for the International Symposium of Medical Information and Communication Technology in 2010. He was the recipient of the Bell Labs Team Award from Lucent Technologies in 2003, the Best Paper Award from the IEEE Vehicular Technology Conference in Fall 2004, and the Outstanding Achievement Award from National Chiao Tung University during 2007–2011.